CHAPTER IV

RESULTS AND DISCUSSION

In today's world, frontier scientific and technological research into the fields of life science, energy, and the environment was interested with the performance, functionality and durability of key materials. The advanced carbon nano-materials play an important role in various applications such as electrochemical, energy storage, sensing, catalysis, transistors and polymer composites.

This thesis was divided into 2 parts; synthesis and application parts, shown in figure 4.1 - 4.2.

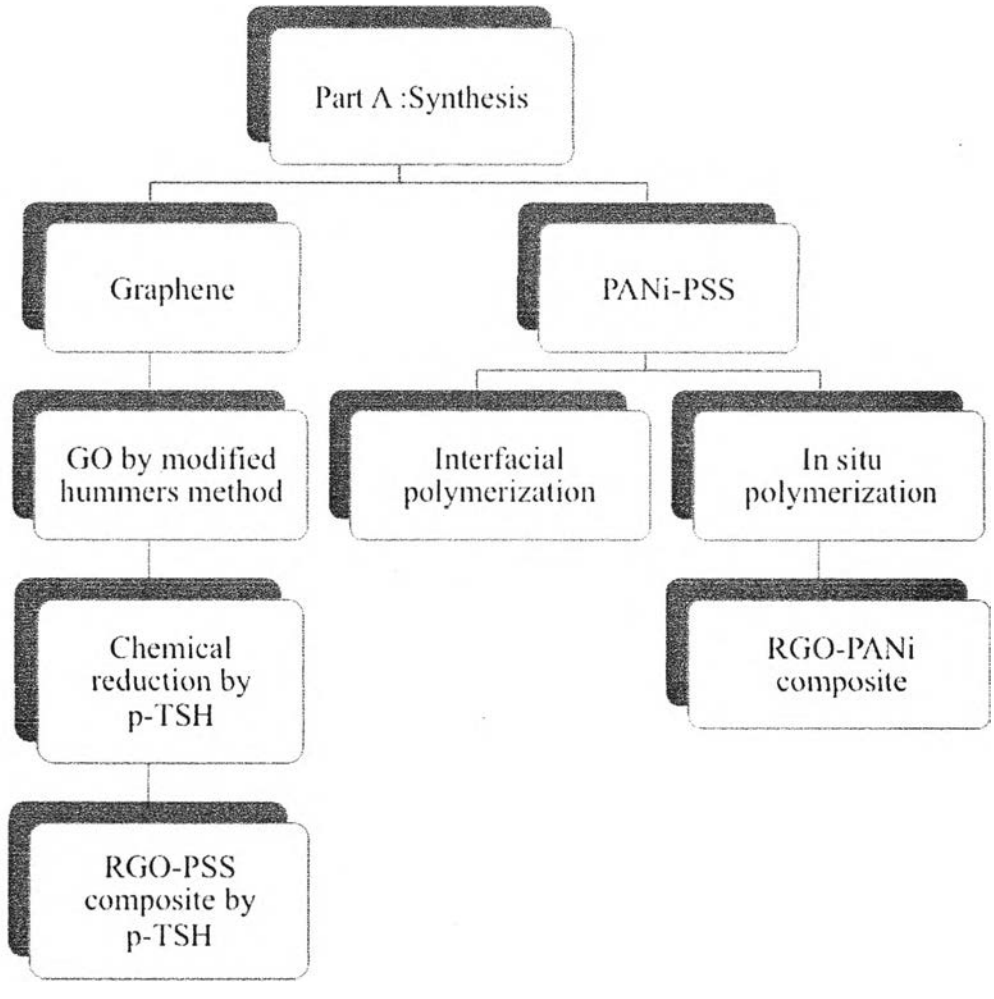

Figure 4.1 The flow chart of part A : The synthesis of graphene and PANi/PSS.

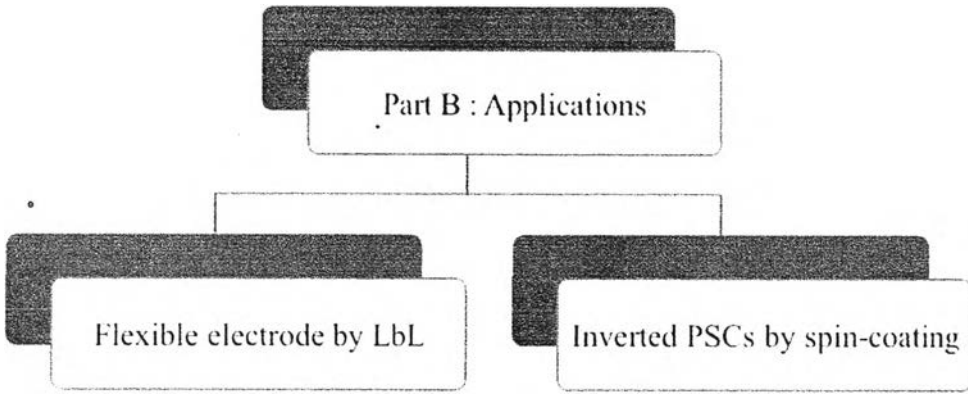

Figure 4.2 The flow chart of part B : The applications of graphene oxide (GO).

One of the advanced carbon nano-material is graphene. Graphene is a 2-dimensional single sheet of carbon atoms arranged in a hexagonal network. It has a large theoretical specific surface area, high intrinsic mobility, high Young's modulus, optical transmittance and good electrical conductivity. Micromechanical cleavage is currently the most effective and reliable method to produce high-quality graphene sheet but low yield production. There are another method ; epitaxial growth, chemical vapor deposition, thermal exfoliation and the chemical reduction of exfoliated graphite oxide. Among these method, graphene can also be prepared at a larger scale by liquid phase exfoliation to form a graphene oxide (GO) intermediate, followed by reduction to restore the graphene structure (RGO), as shown in Figure 4.3.

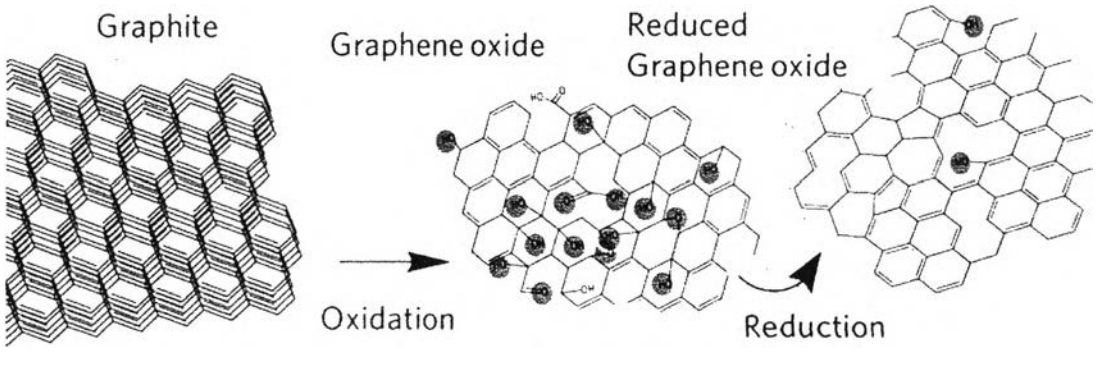

Figure 4.3 The chemical process of graphene oxide.

In general, GO is synthesized by either the Brodie, Staudenmaier or Hummers method. All three methods involve oxidation of graphite to various levels. Brodie and Staudenmaier used a combination of potassium chlorate ($KClO_3$) with nitric acid (HNO_3) to oxidize graphite, and the Hummers method involves treatment of graphite with potassium permanganate ($KMnO_4$), sulfuric acid (H_2SO_4) and sodium nitrate ($NaNO_3$). Hummers method has three important advantages over previous technique. First, the reaction can be completed within few hours. Second, $KClO_3$ was replaced by $KMnO_4$ to improve the reaction safety, avoiding the evolution of explosive ClO_2. Third, the use of $NaNO_3$ instead of fuming HNO_3 eliminates the formation of acid fog. In this work, GO was synthesized by modified Hummers method.

4.1 Part A : Synthesis of GO and RGO

In 2013, Chen and co-workers can be produced GO by improved Hummers method without using $NaNO_3$ for eco-friendly. GO was synthesized from natural graphite powder by a modified Hummer's method without using $NaNO_3$. For their procedure, the mixture was transferred to 95 °C after adding water. We followed this procedure. Unfortunately, GO could not be synthesized from this procedure, GO should be brown color but it changes to dark color after transferring mixture to 95 °C and keep for 15 min. Therefore, temperature is an important factor for synthesis GO. In this work, after adding water, the mixture was still keeping under 45 °C for 1h. Finally, the brown GO gel was obtained follow this procedure and use for synthesis GO.

GO was various ratio of $KMnO_4$ to graphite flake. GO 1:7, 1:8 and 1:9 (G: $KMnO_4$) were brownish gel. The Hummer's method uses a combination of potassium permanganate as oxidant and sulfuric acid as intercalating agent.

During the reaction, Mn_2O_7 is formed according to Equation 4.1 as soon as $KMnO_4$ is added to the dispersion of graphite powder intercalated in concentrated sulfuric acid, observed the dark green color formation immediately after $KMnO_4$ addition.

$$2MnO^-_4 + 2H^+ \longrightarrow Mn_2O_7 + H_2O \qquad 4.1$$

As reported of Dreyer *et al.* in 2010, dimanganese heptoxide (Mn_2O_7) is, in fact, the highly reactive oxidizing agent through permanganate. While bulk Mn_2O_7 decomposes slowly at temperatures around -10°C, it can explode at elevated temperatures exceeding 95°C. This decomposition yields ozone as a byproduct as shown Equation 4.2.

$$4Mn_2O_7 \longrightarrow 8MnO_2 + 2nO_3 + (6-3n)O_2 \quad ; (0 < n < 2) \qquad 4.2$$

After completing the oxidation, Mn_2O_7 was quenched with DI water following by Equation 4.3

$$Mn_2O_7 + H_2O \longrightarrow HMnO_4 \qquad 4.3$$

The decomposition of Mn_2O_7 leads to MnO_2 , which is insoluble in water. To remove manganese impurities, MnO_2 and MnO_4^- are reduced to form soluble Mn^{2+} salts by addition of H_2O_2 to the acidic solution (Equations 4.4 - 4.5).

$$MnO_2 + H_2O_2 + 2H^+ \longrightarrow Mn^{2+} + O_2 + 2H_2O \qquad 4.4$$

$$2MnO_4^- + 5H_2O_2 + 6H^+ \longrightarrow 2Mn^{2+} + 5O_2 + 8H_2O \qquad 4.5$$

Figure 4.4 plots the XRD pattern of Graphite flake, GO 1:5, GO 1:7 and GO 1:9. The results of graphite flake shows strong reflection at 26.54°, following 44.63° and 54.75°. After oxidation, all of the GOs (1:5, 1:7 and 1:9) exhibit the diffraction peak shift to a lower 2θ angle at 10.89° and 42.46, indicating a interlayer spacing approximately 0.87 nm. This indicated the GO sheets are separated due to the covalently bonded oxygen. The oxidation of graphite flake with $KMnO_4$ to GO disrupts the conjugation of the graphene structure resulting a decrease electronic conductivity.

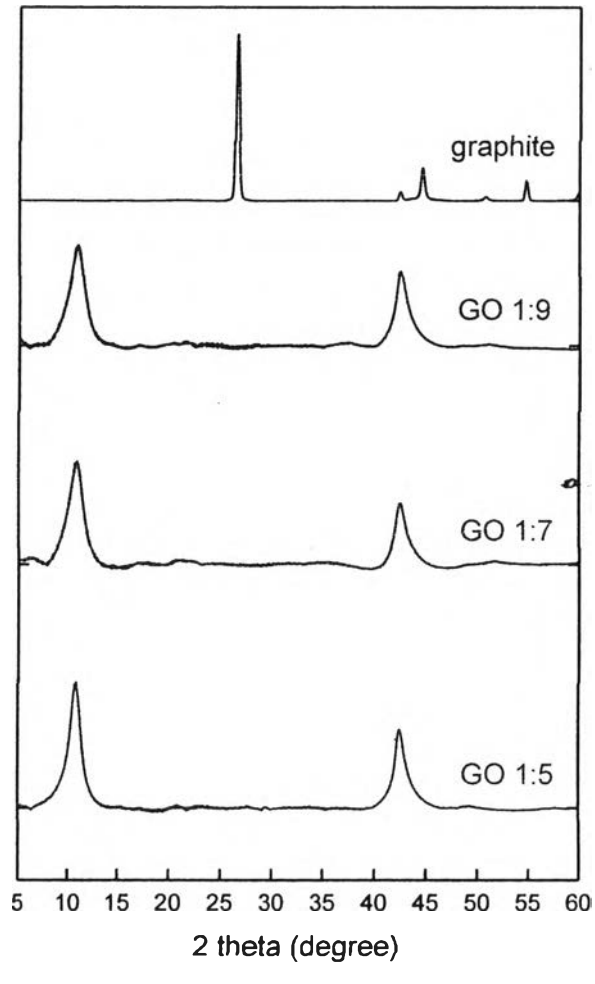

Figure 4.4 Shows XRD pattern of graphite powder and GOs.

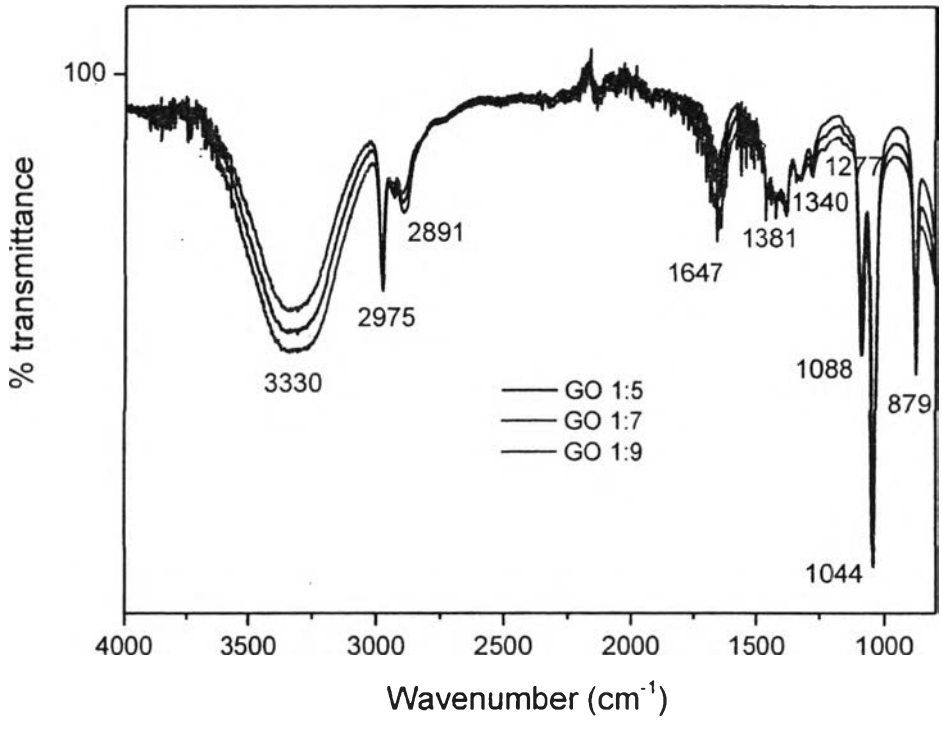

Figure 4.5 The FTIR spectra of GOs samples (1:5, 1:7 and 1:9)

The FTIR spectra of GO 1:5, 1:7 and 1:9 are shown in Figure 4.5. For all GOs, the peaks indicated as C-OH bonding at 3326 cm^{-1} with broad peak from hydroxyls and trapped water molecules and a sharp peak at 2971 cm^{-1} for C-H bonds. The others peaks are 1650 cm^{-1} related to C=C bonds from unoxidized sp^2 graphite domains, 1382 cm^{-1} attributed to O-H deformation (C-OH or carboxyl group), 1087 cm^{-1} due to C-O (epoxy or alkoxy) stretching. GO 1:7 show the highest %tranmittance which indicated that there are many functional groups in this GO. This ratio is suitable to use for synthesis of GO due to high functional group. Therefore, it can be fabricated easily with polymer that contain positive charge such as PDADMAC.

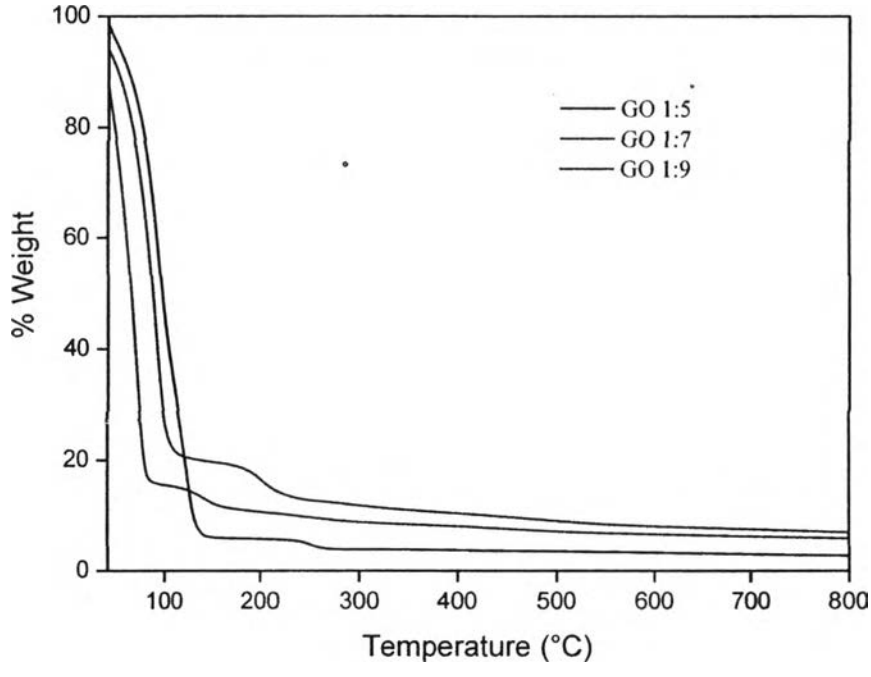

Figure 4.6 TGA thermograms of GO 1:5, 1:7 and 1:9.

From the TGA thermograms, the first mass decrement up to 100°C is ascribed to the evaporation of water molecules and the second was decrement between 180° and 200° which corresponses to CO, CO_2 and residual water molecules. Mass retention ratios for GO 1:5, 1:7 and 1:9 are 7, 11 and 9.5 % , respectively as shown in Fig 4.6. At the second loss, GO 1:7 has more loss functional group than 1:9 and 1:5, related to the ratio 1:7 of graphite flakes to $KMnO_4$ is suitable to use for synthesis GO.

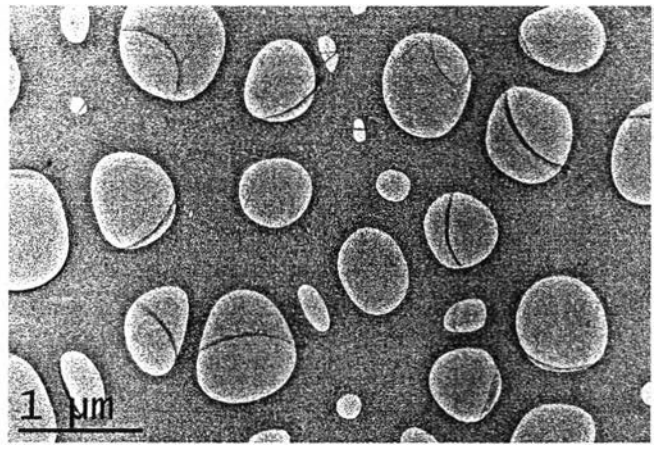

Figure 4.7 TEM image of GO.

The surface topological measurement of GO was performed under ambient condition by transmission electron microscopy (TEM). TEM result as shown in Figure 4.7 demonstrated the single layer of graphene oxide sheet on copper grid with holey carbon. This GO synthesized from 1:7 ratio and this procedure can completely exfoliate graphite flake to graphene oxide sheet.

The polar oxygen functional groups of GO make it hydrophilic. GO can be exfoliated in many solvents, and disperses in water. Dispersions of graphene oxide can be obtained by stirring and sonication of GO in solvents. Chemical reduction of the GO colloidal dispersions was use to restore the structure of GO resulting the electrical conductivity of RGO. There are several reducing agents, such as hydrazine, hydroquinone, sodium borohydride ($NaBH_4$) and ascorbic acid. However, RGO turned to agglomerate and precipitation after reduction. To avoid this problem, Yun J.-M and co-workers reported a newly conversion GO to RGO by using p-toluenesulfonyl hyhrazide (p-TSH).

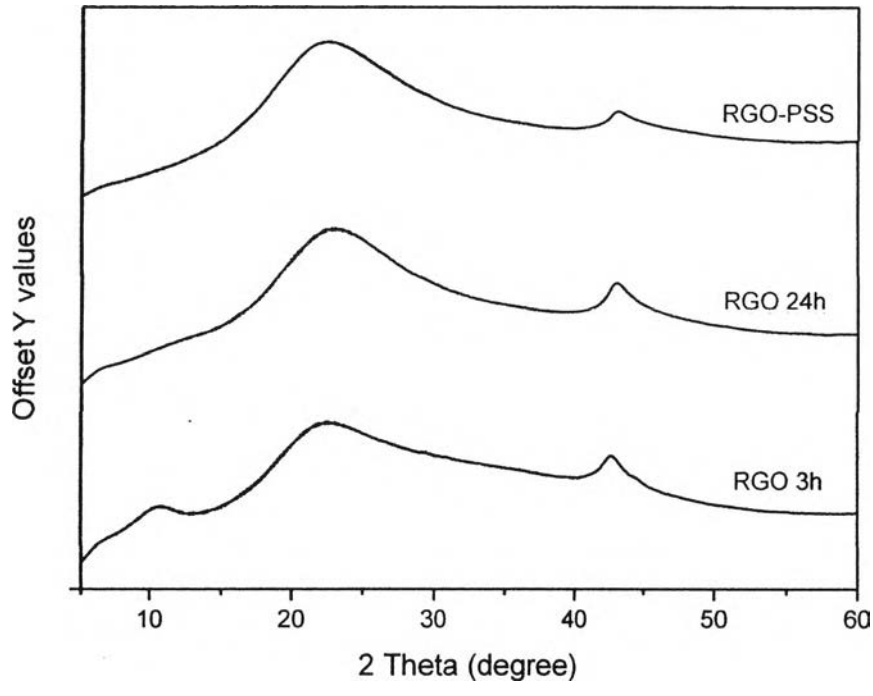

Figure 4.8 XRD characterization of RGO 3h, RGO 24h and RGO-PSS.

Therefore, we synthesized RGO by using p-TSH chemical reduction by 3 h and 24 h. RGO, reduced for 3 h, showed reflection at 10.70°, 22.32° and 42.66° in Figure 4.8. While the peaks of RGO reduced for 24 h appear at 22.86° and 43.02° similar with RGO-PSS. We could summarize that RGO 3h is partially RGO due to residual functional groups inside GO sheet and fully RGO was prepared by reduction of GO for 24 h.

PSS is a strong polyelectrolyte which completely dissociate to ion pairs in water. This electrostatic charges are localized on PSS backbone whereas the numerous oppositely charged counter ions are distributed in the solution, thus gain entropy. Therefore, this conformation helps to minimize the repulsive electrostatic interaction between the equally charged functional groups of $-SO_3H$ in the polymer backbone.

4.2 Part A : Synthesis of PANi-PSS and RGO-PANi Composite

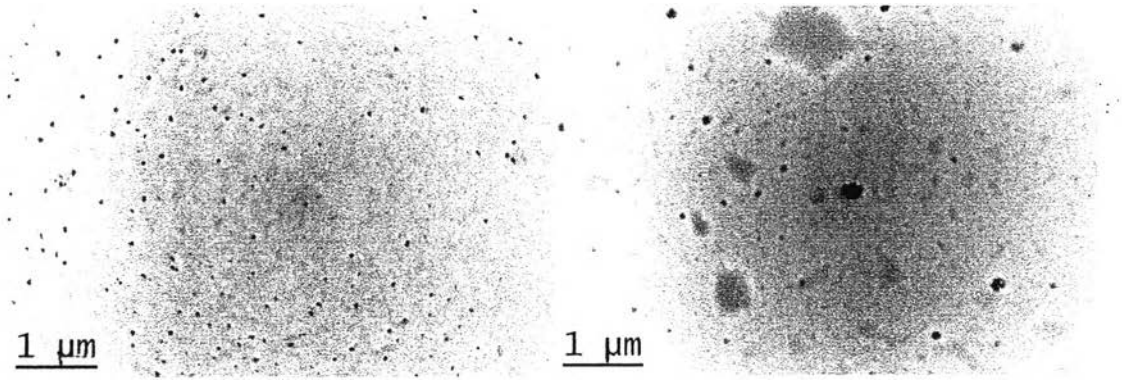

Figure 4.9 TEM image of PANi-PSS composite in 0.1 M HCl acid(a) and 1 M HCl acid (b).

Polyaniline was prepared by interfacial polymerization with PSS using 0.1 and 1 M HCl acid. After polymerization for 24 h, PANi-PSS composite was studied topology by transmission electron microscopy (TEM). Figure 4.9 shows TEM image of polyaniline synthesized in 0.1 M HCl acid (a) and 1 M HCl acid (b). The particle size of PANi-PSS from 1 M HCl acid were larger than PANi-PSS from 0.1 M HCl. Moreover, the large particles in 1 M HCl precipitate from the dispersion while the small particles from 0.1 M HCl formed stable colloids in water. As this result, pH is an important factor for synthesis of PANi-PSS composite and affect to stability of the dispersion. The pKa of poly(4-styrenesulfonic acid) is approximately 1.0. At pH <1, the sodium 4-styrenesulfonate groups on PSS are converted to electrically-neutral 4 – stryrenesulfonic acid groups. Due to the small number of negatve charged sites on PSS, polymerization of aniline resulted in PANI polymers that loosely anchored on PSS template, which results in larger PANi-PSS composite particles. When pH>1, the styrenesulfonic groups on PSS are in the salt form, so size of the particles is not affected by pH, (Li *et al.* 2012).

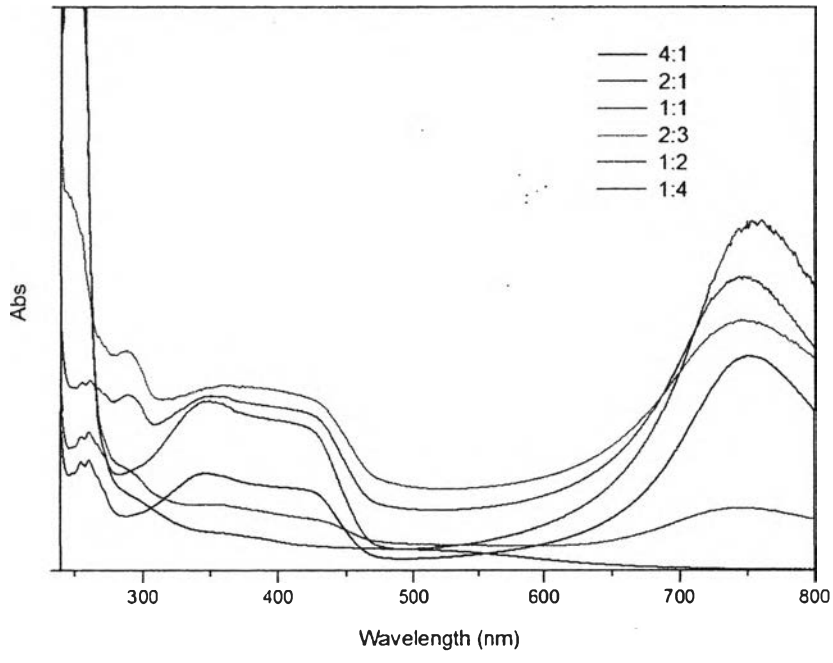

Figure 4.10 The UV spectra of PANi-PSS composite from various molar ratio of APS and aniline monomer (APS : ANi).

To synthesize polyaniline on PSS as template, Ammoniumpersulfate oxidant was studied for the suitable molar feed ratio with aniline monomer. The molar ratio of APS:ANi which are 4:1, 2:1, 1:1, 1:1.5, 1:2 and1:4 were used to synthesize PANi-PSS by interfacial polymerization using 0.1 M HCl acid. After polymerization for 24 h, the dispersion of PANi-PSS composite was characterized by UV-Vis spectrophotometer. The result shown as Figure 4.10 indicates that the PANi-PSS composite yield increase at 4:1 and show the highest yield at 2:1 molar ratio of APS:ANi. After 2:1 ratio, PANi-PSS composite keep decreasing until 1:4 molar ratio.

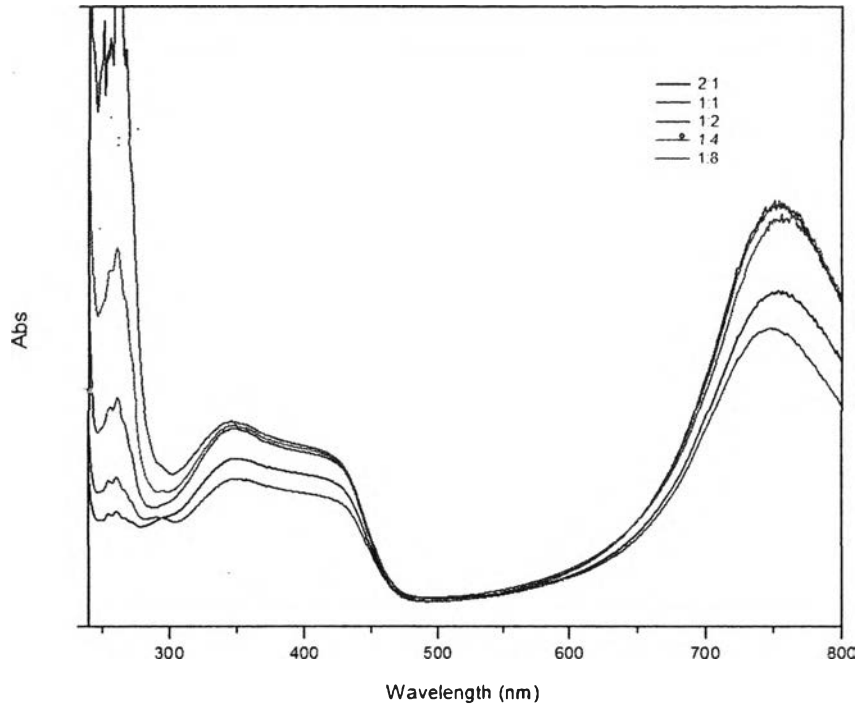

Figure 4.11 The UV spectra of PANi-PSS composite from various molar ratio of APS and aniline monomer (APS : ANi).

Not only APS but also PSS was studied the effect of synthesis of polyaniline on PSS template. In 2011, Chung and co-worker showed the effect on size of PANi-PSS composite. The molar ratio of ANi is higher than PSS resulting PANi particles experienced an unsaturated doping state of PANi-PSS. A large number of ANi monomers were adsorbed through the electrostatic interaction onto fewer SO_3^- groups of PSS interface. After that the polymerization of the higher concentration of absorbed ANi monomer changed to network PANi by APS and joined with the polymer matrixs. When the molar ratio of PSS was higher than ANi monomer, the low concentration of adsorbed ANi monomers turned into nanoparticle or short rods of PANi-PSS composite.

In this work, the molar ratio of ANI:PSS was varied to 2:1, 1:1, 1:2, 1:4 and 1:8. At molar ratio 1:2,1:4, 1:8 of ANi:PSS shows the similar highest absorbance but show higher absorbance of PSS absorption peak around 225 and 261 at higher molar ratio of PSS, as shown in Figure 4.11. The molar ratio 1:2 of PANi-PSS was enough to synthesize PANi-PSS cómposite. The PANi-PSS from 2:1 molar ratio precipitated to the interface due to less amount of PSS to stabilize PANi to disperse in water. on the other hand, the PANi-PSS from the malar ratio 1:1, 1:2, 1:4 amd 1:8 can disperse well in water phase.

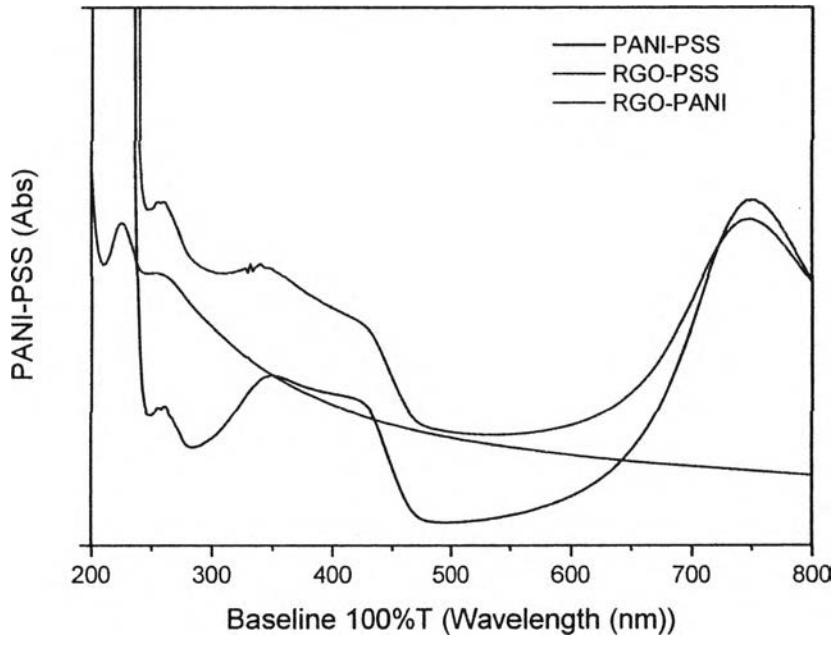

Figure 4.12 UV-Vis spectra results of PANi-PSS, RGO-PSS and RGO-PANi composite.

Here, we synthesized the water-dispersible PANI-PSS by in situ polymerization in 0.1 M HCl. The aniline monomers joined with PSS changed into PANi network by APS. The 2:2:1 molar feed ratio of ANi:PSS:APS was used in this synthesis. The water-dispersible PANi-PSS is green solution. Fig. 4.12 Shows UV-Vis absorption spectra of PANi-PSS in 0.1 M HCl. The PANi-PSS composite have broad peak between 310 and 450 nm, related to π-π^* transition in PANi, and main adsorption peak centered at 750 nm, corresponded to the polaron structure of the main chains of PANi. There are two adsorption peaks at 225 and 261 nm of PSS. After modification PANi and RGO with PSS, two absorption peaks appear at 225 and 261 nm which indicates that PSS molecules are completely attached with PANi and RGO.

The RGO-PANi composite was prepared by physical mixing of PANI-PSS and RGO-PSS. After preparation, the absorbance at broad peak at 310 and 450 nm of RGO-PANi increases due to π-π interaction between π orbital of conjugated structure in PANi and π orbital in the structure of RGO sheet, resulting from physical bonding.

4.3 Part B : Application of GO

4.3.1 Flexible Thin Film Electrode of RGO/PDADMAC by LbL Assembly Technique.

GOs, synthesized with different ratio of $KMnO_4$; 1:1, 1:3, 1:5, 1:7 and 1:9, were used to do LbL technique. Before preparation of thin film, each GO was dispersed in 0.1 M NaOH and sonicated for 1 h, resulting partially RGO under alkaline solution. Alkaline reduction of GO can overcome many limitation of RGO such as high toxicity, hazardous bi-product and aggregation of RGO.

In 2012, Sanjaya *et al.* reported that, after the alkaline reduction, the size of the undisrupted sp^2 do mains of GO did not change dramatically. This process converts carboxylic groups to negative charged carboxylate groups, so the negatively charged particles do not agglomerate when the GO sheets was reduced.

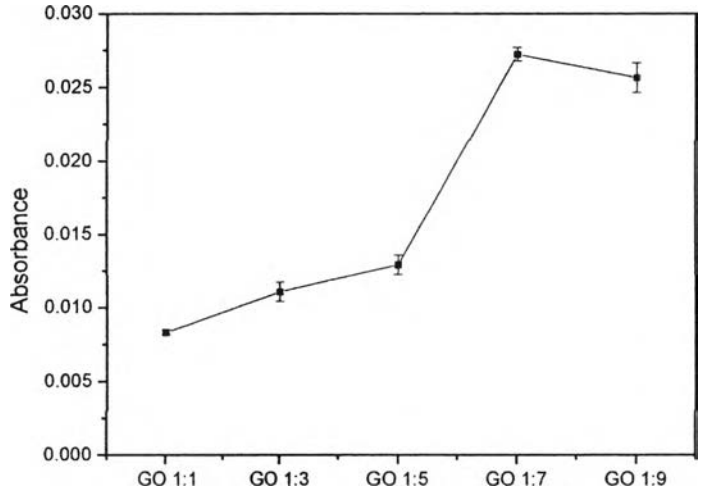

Figure 4.13 Graph plots between absorbance at 550 nm and RGO prepared from different GOs.

The primer-coated glass substrates was dip into each RGO alkaline solution for preparing thin film. RGO/PDADMAC composite films were characterized with UV-Vis spectrophotometry. At wavelength 550 nm, RGO which prepared by 1:7 demonstrates the highest absorbance (Figure 4.13); therefore, this ratio is the suitable ratio to use to prepare RGO for LbL technique.

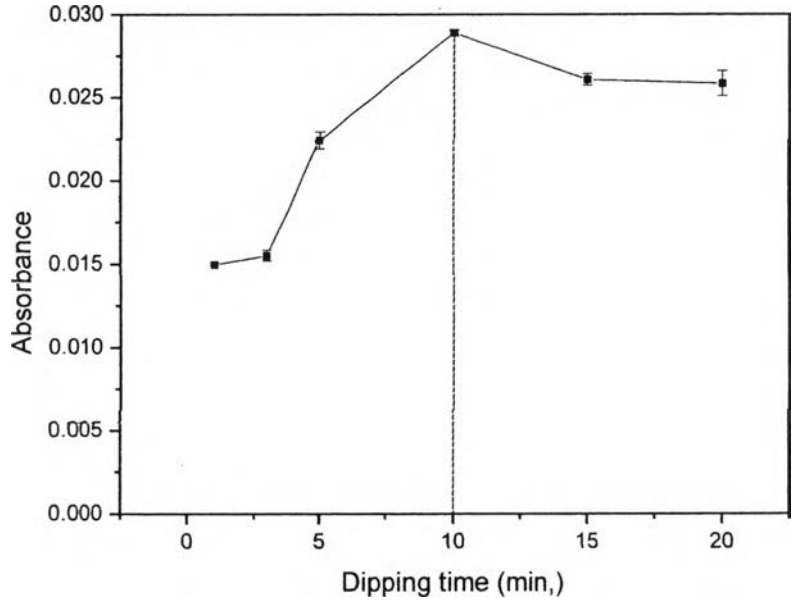

Figure 4.14 Effect of dipping time of RGO for LbL technique.

RGO prepared by GO1:7 ratio was used to study the suitable dipping time which RGO can stick maximum and measured it by UV-Vis spectrophotometry at 550 nm. The dipping time was varied to 1, 3, 5, 10,15 and 20 min respectively. In Figure 4.14 shows the highest absorbance at 10 min dipping time and slowly decrease after 10 min. Morover, pH parameter was studied at pH 2, 4, 6, 8, 9, 10, 11, 12, 13 and 14. At pH below 7, GO can precipitate like cloudy in acid condition which affect film is not smooth because of small particle distributed on glass slide.

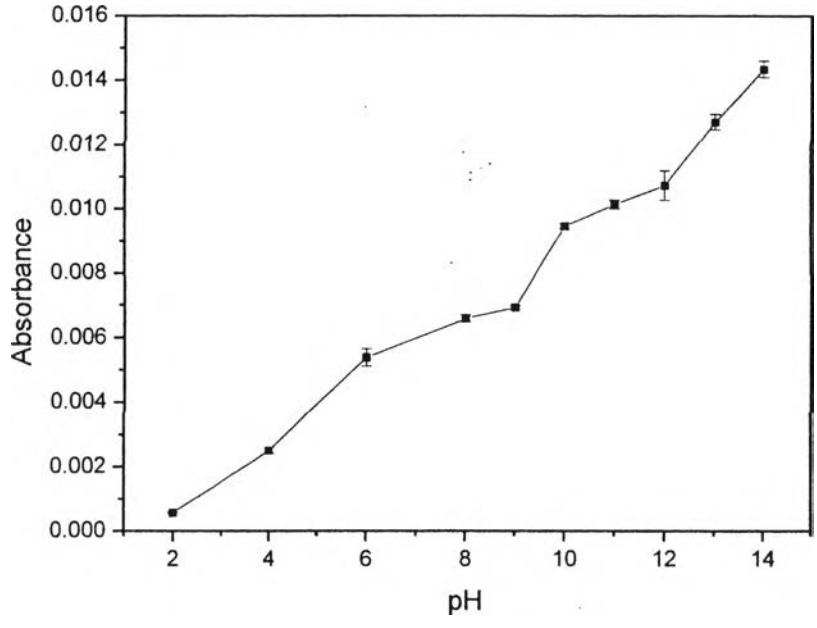

Figure 4.15 pH parameter was studied for LbL technique.

On the other hand, GO can disperse well in base condition, pH above 7. The GO become black solution of RGO when disperses it in higher pH and can be deposited on substrates proportional with increasing pH value (shown as Figure 4.15) which distributed to effect of alkaline concentration reduction. It is implied that the extensive conjugated sp^2-carbon network is restored in the NaOH or alkaline solution.

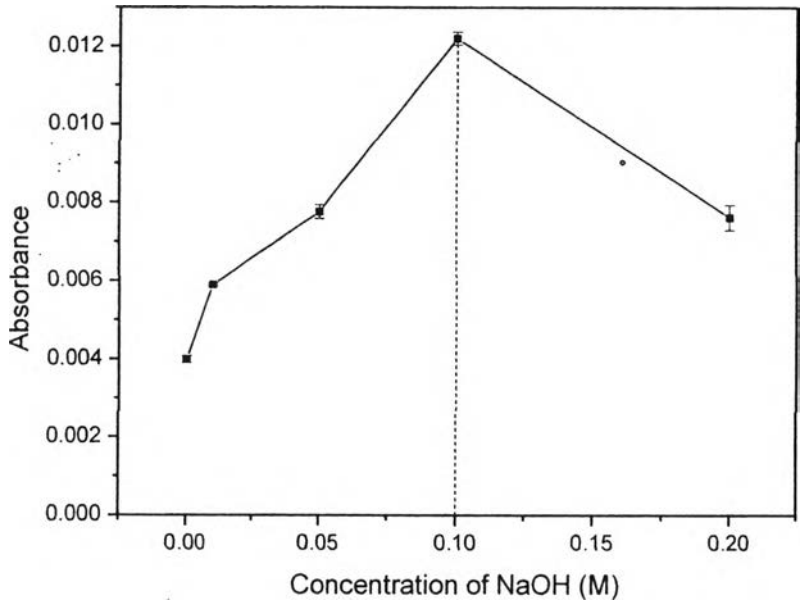

Figure 4.16 Effect of alkaline concentration reduction of RGO for LbL technique.

RGO was prepared under 0.01, 0.05, 0.1, 0.2, 0.5 and 1 M NaOH. The results show the maximum absorbance when RGO was reduced by 0.1 M NaOH and gradually decrease in higher concentration (Figure 4.16). RGO started to agglomerate at 0.2 M NaOH result in defect on composite film. It suggested that the higher concentration of alkaline solution, the higher reduction. RGO decrease the sheet size affected to agglomerate RGO in solution.

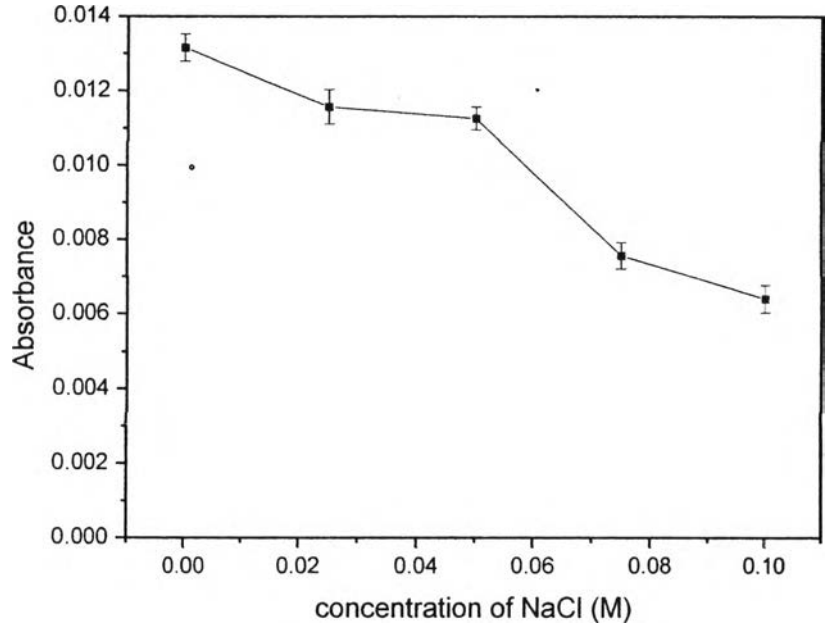

Figure 4.17 Effect of salt concentration parameter for LbL technique.

From literature review, salt increases efficiency of LbL technique because of screen repulsion charge between ion and affect to sample can stick better. from this reason, we have studied to increase the efficiency of GO film by adding NaCl into GO solution. The various concentrations of NaCl ; 0.025M , 0.050M , 0.075M and 0.100M, were added in 0.2 mg/ml RGO solution. The absorbance decreasing with adding NaCl as shown in Figure 4.17. Obviously, GO will precipitate at 0.050 M of NaCl. Therefore, salt is not necessary for LBL technique of GO. For polymer, electrostatic charges of salt can stabilize along polymer chain affected to increase efficiency of deposition while RGO is sheet which has negative charge at edge and basal plane. When positive charge stabilize to RGO, each RGO sheet could be closer and form large particle like agglomeration. Loading amount of RGO are shown in Figure 4.18. The highest amount of RGO can be deposited on substrate is 5 mg/ml.

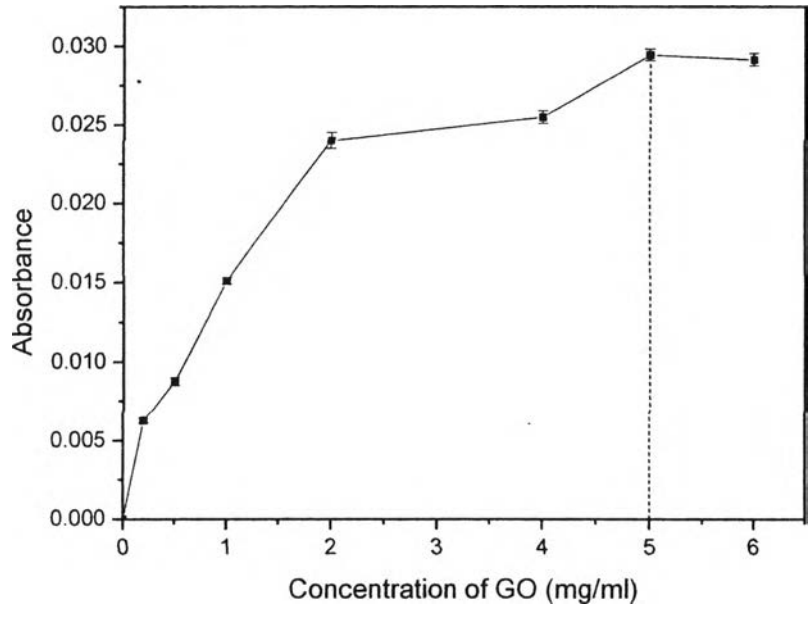

Figure 4.18 Loading amount of RGO for LbL technique.

4.3.2 RGO/PANi Composite as Interfacial Hole Transport Layers for Inverted PSCs.

RGO/PANi composite was use as interfacial HTL layers for inverted PSCs. From the contact angle measurement of various layers shown in Figure 4.19, it can be measured contact angle values of 98.3° for PEDOT:PSS and PTB7:$PC_{71}BM$ layer. However, the contact angle was found to decreased to 13.1° when RGO/PANi was deposited on PEDOT:PSS. The contact angle of RGO/PANi composite on PTB7:$PC_{71}BM$ is 75.5° which be less than PEDOT:PSS. As this result, RGO/PANi composite was found to increase the wettability of PEDOT:PSS on active layer which is very interesting for the fabrication of solar cells using the spin coating method.

(b)

(c)

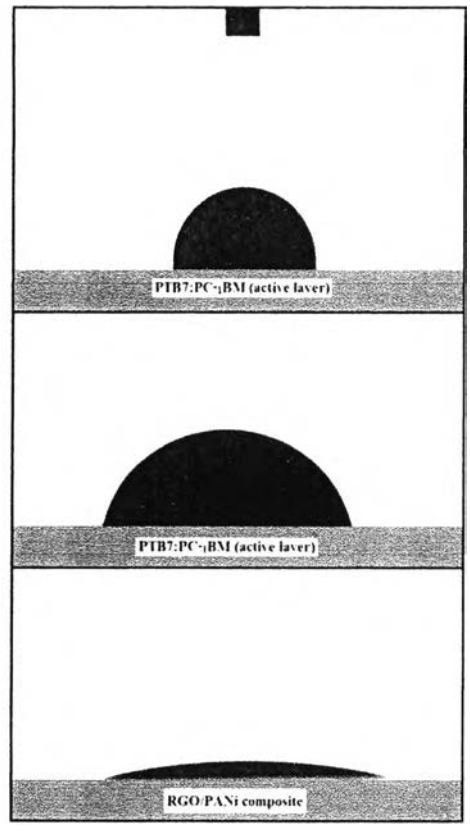

Figure 4.19 The contact angle of (a) PEDOT:PSS (HTL) and (b) RGO/PANi on PTB7:$PC_{71}BM$ as active layer , (c) PEDOT:PSS on RGO/PANi composite by using glass slide substrate.

Moreover, the electrical conductivity of materials used in PSCs are the important factor. The electrical conductivity was measured by TLM method. Figure 4.20 shows the plots between resistance and channel length of PANi-PSS, RGO-PSS and RGO/PANi composite. At 0.002 cm of channel length, RGO-PSS and PANi-PSS show resistance 18.02 and 19.37 ($x10^5$) Ohms respectively. It shows that RGO-PSS has lower resistance than PANi-PSS. After mixing RGO-PSS and PANi-PSS composite, RGO-PANi composite show higher resistance compare with RGO-PSS. An increasing of resistance of RGO-PANI composite may result from a high amout of PSS in composite because PSS is an insulating polymer. In each composite, RGO-PSS and PANi-PSS, has high amout of PSS to improve dispersibility. However, this solution can well dispersed in water phase , the conductivity was decreased. In polymer solar cells, conductivity of material are the important factor to consider the material for apply to device.

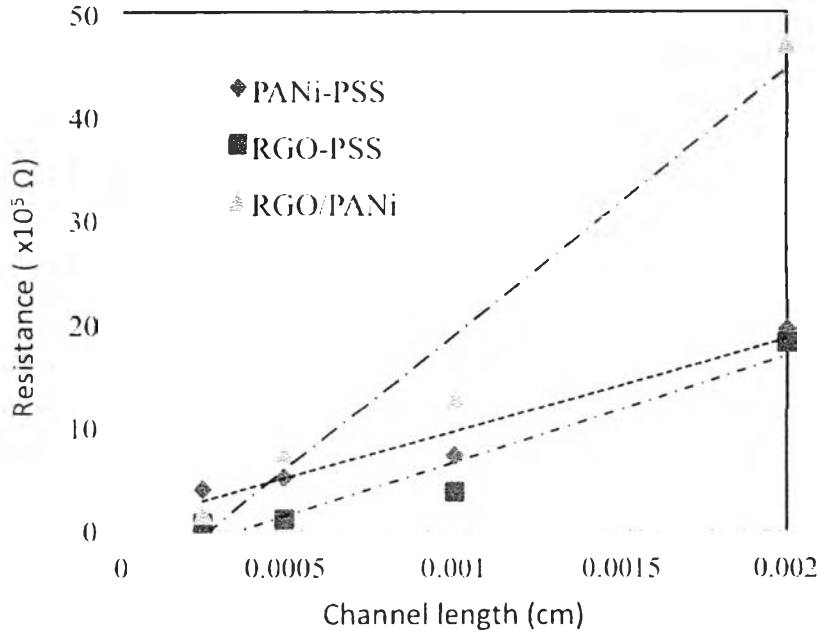

Fig.4.20 Shows the plots between resistance and channel length of PANi-PSS, RGO-PSS and RGO/PANi composite.